How do the water vapor and carbon monoxide "tape recorders" start near the tropical tropopause?

Chuntao Liu,[1] Ed Zipser,[1] Tim Garrett,[1] Jonathan H. Jiang,[2] and Hui Su[2]

[1] This paper evaluates geo-seasonal relationships in tropical deep convection using radar and infrared data from Tropical Rainfall Measuring Mission (TRMM), near tropopause thin clouds from Stratospheric Air and Gas Experiment (SAGE) II, water vapor and carbon monoxide (CO) from the Earth Observing System (EOS) Microwave Limb Sounder (MLS), and the tropopause temperature from National Center of Environment Prediction (NCEP) reanalysis data. Geo-seasonal variations in MLS water vapor at 146 hPa and 100 hPa are negatively correlated, which points to dehydration at the tropical tropopause. Water vapor at 146 hPa is highly correlated with tropical deep convection and thin clouds, but at 100 hPa it is more highly correlated with the tropopause temperature. There is a high correlation between the geo-seasonal variations of $14-16$ km thin cloud and cold clouds from deep convection. However, at $16-18$ km, thin clouds are highly correlated with the tropopause temperature as well as with deep convection. There is a semi-annual cycle in CO concentrations at 100 hPa and 146 hPa. The variability is consistent with the convolved seasonal variation of deep convection and surface biomass burning. The annual cycle of water vapor at 100 hPa correlates with the seasonal variability of "freezing and drying" between 146 hPa and 100 hPa, which in turn correlates with changes in tropopause temperature associated with deep convective lifting or large scale ascent. **Citation:** Liu, C., E. Zipser, T. Garrett, J. H. Jiang, and H. Su (2007), How do the water vapor and carbon monoxide "tape recorders" start near the tropical tropopause?, *Geophys. Res. Lett.*, *34*, L09804, doi:10.1029/2006GL029234.

1. Introduction

[2] A detailed mechanism for explaining dehydration of air ascending from troposphere into the stratosphere remains under debate. While the "freeze and dry" concept [*Brewer*, 1949] has been generally accepted, two main explanations have been offered. One is that tropical deep convection dehydrates air when it reaches or penetrates the tropical tropopause [*Danielsen*, 1982; *Newell and Gould-Stewart*, 1981; *Sherwood and Dessler*, 2000; *Su et al.*, 2006]. Another is that when air ascends through the upper troposphere, water substance freezes and makes it dry [*Hartmann et al.*, 2001; *Holton and Gettelman*, 2001; *Jensen and Pfister*, 2004]. Since ice cloud is direct evidence of freezing, thin ice clouds near the tropical tropopause are the subject of many studies

[*Jensen et al.*, 1996; *Wang et al.*, 1996; *Sandor et al.*, 2000; *McFarquhar et al.*, 2000; *Massie et al.*, 2002]. Many studies show that there is good spatial correlation between these thin clouds and deep convection [*Massie et al.*, 2002; *Dessler et al.*, 2006; *Liu*, 2007].

[3] Carbon monoxide (CO) has a photochemical life time of weeks to months in the troposphere and is often used as a tracer for vertical and horizontal transport near the tropopause [e.g., *Kar et al.*, 2004]. Since CO is insoluble and immune from the dehydration process, it can be used to facilitate understanding of the driving mechanisms behind water vapor concentrations near the tropopause. Following the discovery of an atmospheric "tape recorder" that tracks the gradual upward propagation of water vapor in the stratosphere [*Mote et al.*, 1996], subsequent observations from the Earth Observing System (EOS) Microwave Limb Sounder (MLS) have shown a corresponding carbon monoxide (CO) "tape recorder." In general, CO and water vapor are negatively correlated in the lower stratosphere [*Schoeberl et al.*, 2006]. However, there is an important difference between the seasonal cycles of the near tropopause heads of the water vapor and CO tape recorders. Whereas the water vapor tape recorder follows an annual cycle, the CO signal follows a semi-annual cycle between 146 and 100 hPa (Figure 1) with low CO in January, July, and August. Relatively low CO early in the year is especially obvious in 2006.

[4] This study is motivated by the following questions: (1) What are the relationships between deep convection, thin clouds, water vapor, and CO near the tropical tropopause? (2) In particular, what accounts for observed differences between the seasonal cycles in CO and water vapor within the $100-146$ hPa layer?

[5] To answer the above questions, we combine observations from the Tropical Rainfall Measuring Mission (TRMM) [*Kummerow et al.*, 1998], the Stratospheric Air and Gas Experiment (SAGE) II [*McCormick et al.*, 1993], and the EOS MLS. Geo-seasonal cycles of selected parameters representing the deep convection, thin clouds, water vapor, and CO near tropical tropopause are compared with the geo-seasonal cycles of tropopause temperature from (NCEP) reanalysis data [*Kistler et al.*, 2001] as well as CO surface emission rates from the global emissions inventory described by *Duncan et al.* [2003]. Section 2 of this paper introduces the data and the analysis methods. Section 3 presents the geo-seasonal cycles of these parameters and their correlations. Section 4 discusses the results.

2. Data and Methods

[6] In prior literature, satellite observations of deep convection reaching the tropical tropopause have been

---

[1]Department of Meteorology, University of Utah, Salt Lake City, Utah, USA.

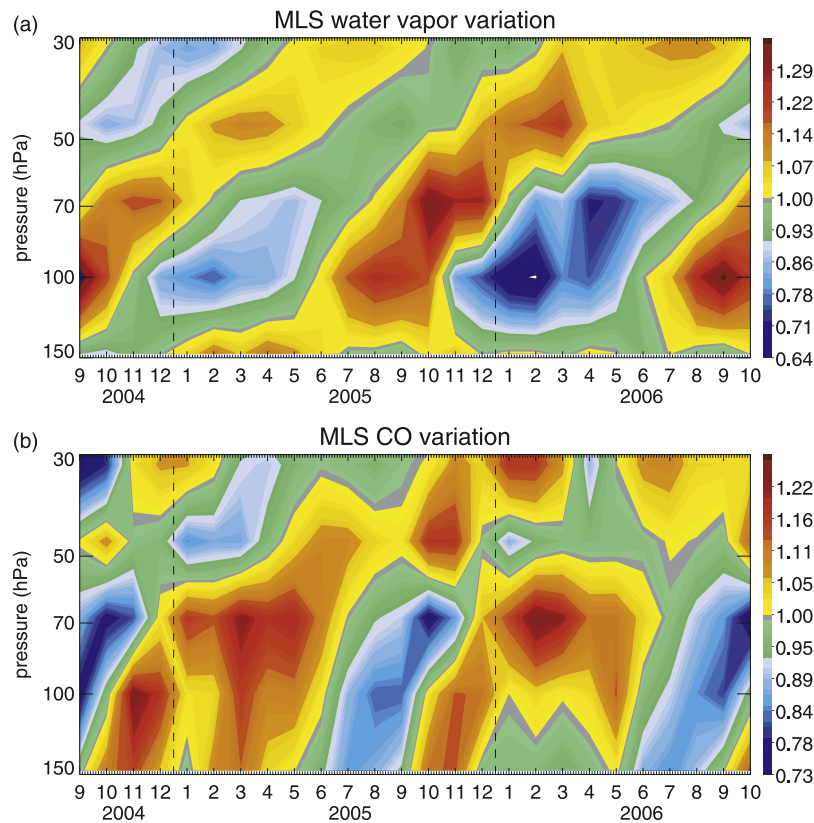[2]Jet Propulsion Laboratory, California Institute of Technology, Pasadena, California, USA.

Figure 1. (a) Seasonal variation of $10°N-10°S$ mean EOS MLS water vapor after dividing by the mean value at each level. (b) Seasonal variation of $10°N-10°S$ EOS MLS CO after dividing by the mean value at each level.

represented in two principal ways. The first is by the area of clouds with low infrared brightness temperatures [*Gettelman et al.*, 2002; *Massie et al.*, 2002; *Liu et al.*, 2007]. The second is by the area of radar echoes reaching the tropopause [*Alcala and Dessler*, 2002; *Liu and Zipser*, 2005]. In this study, we examine the areas of clouds that have TRMM Visible and Infrared Scanner (VIRS) 10.8 μm brightness temperatures colder than 210 K, and the area of 20 dBZ echoes at 14 km measured by the TRMM Precipitation Radar (PR). The year studied is 2005. To generate geo-seasonal distributions of deep convection near the tropical tropopause, the areas of VIRS cold clouds and PR echoes at 14 km from $10°S-10°N$ are accumulated in $10°$ longitude boxes for each month. Geo-seasonal distributions are obtained from the ratio of the accumulated area to total area in each box.

[7] Thin cloud occurrence near the tropopause is obtained from SAGE II observations. An algorithm similar to the SAGE II cloud detecting algorithm developed by *Kent et al.* [1993] is used, which infers the presence of cloud when the 1.02 μm extinction coefficient is greater than 0.001 km^{-1}, and the ratio of 0.525 μm extinction coefficient to the 1.02 μm extinction coefficient is greater than 0.95. Subvisual clouds near the tropopause are identified from version 6.2 SAGE II data from 1985–2004, excluding the years 1991–1995 which were contaminated by volcanic aerosol [*McCormick et al.*, 1995]. Mean cloud occurrences are calculated as the percentage of events with clouds in two layers (14–16 km and 16–18 km) from $10°N-10°S$ and in $10°$ longitude boxes.

[8] Concentrations of water vapor and CO near the tropical tropopause are available from retrievals of EOS MLS measurements [*Livesey et al.*, 2005, 2006]. Monthly mean water vapor and CO mixing ratios at 146 hPa and 100 hPa in the $10°N-10°S$ and $10°$ longitude boxes are calculated from one full year (2005) of version 1.5 MLS retrievals. In this work, all MLS data are processed with requirements described by *Livesey et al.* [2005]. Tropopause temperature is averaged from the $2.5°$ resolution NCEP reanalysis data [*Kistler et al.*, 2001; *Randel et al.*, 2004] in 2005. Similarly, the geo-seasonal variation of GEIA CO surface emission rate in 2005 is averaged in the same $10°N-10°S$ and $10°$ longitude boxes in each month.

3. Results

[9] Figure 2 shows the geo-seasonal variations of deep convection, thin cloud, water vapor, CO, and tropopause temperature. The incidence of cold cloud reaching 210 K (Figure 2a) shows four persistent longitudinal bands. These are located over the west Pacific ($150°E-180°E$), western Indonesia ($90°E-120°E$), central Africa ($10°E-35°E$) and the Amazon ($50°W-80°W$). The latter three locations display maximum incidence in Spring and Fall. The disproportionately small area of 20 dBZ radar echoes reaching 14 km over the West Pacific in Figure 2b is probably due to the relatively smaller or less particles inside the relatively weak deep convection over the region [*Liu et al.*, 2007]. Notably, the geo-seasonal pattern in deep convection is similar to climatology of geo-seasonal
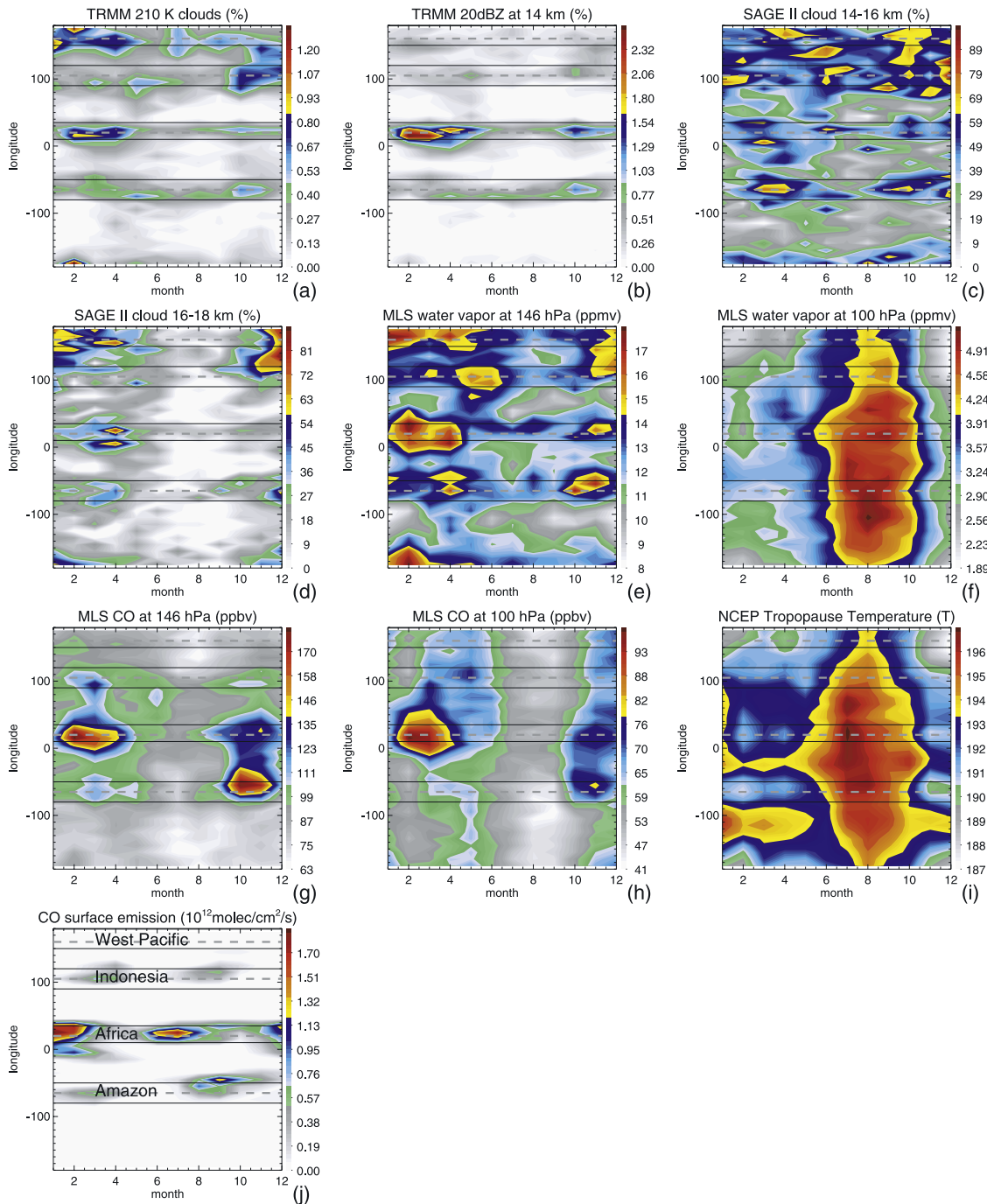
Figure 2. (a) Monthly mean of 10°S–10°N longitudinal distribution of area with TRMM VIRS 10.8 μm brightness temperature < 210 K in 2005. Total values add up to 100%. Four regions of focus over the west Pacific (150°E–180°E), western Indonesia (90°E–120°E), central Africa (10°E–35°E) and the Amazon (50°W–80°W) are boxed. (b) Same as Figure 2a, but for area of TRMM PR 20 dBZ reaching 14 km in 2005. (c) A 10°S–10°N longitudinal variation of monthly cloud occurrence at 14–16 km from 17 years SAGE II data. (d) Same as Figure 2c, but for SAGE II cloud occurrence at 16–18 km. (e) A 10°S–10°N longitudinal variation of monthly mean of MLS water vapor mixing ratio at 146 hPa in 2005. (f) Same as Figure 2e, but for MLS water vapor mixing ratio at 100 hPa in 2005. (g) Same as Figure 2e but for MLS CO mixing ratio at 146 hPa in 2005. (h) Same as Figure 2e but for MLS CO mixing ratio at 100 hPa in 2005. (i) Same as Figure 2e but for NCEP reanalysis tropopause temperature in 2005. (j) Same as Figure 2e but for mean CO surface emission rate.

variations in thin cloud occurrence near the tropopause (Figures 2c and 2d).

[10] The negative correlated geo-seasonal cycles of water vapor at 100 hPa (Figure 2f) and 146 hPa (Figure 2e) are consistent with the tape head locations suggested by *Read et al.* [2004]. The geo-seasonal variation of MLS water vapor at 146 hPa shows the similar pattern of four bands as is seen with deep convection in Figure 2a. This is consistent with

Table 1. Correlation Coefficients Among Geo-Seasonal Distributions of TRMM Proxies for Deep Convection, SAGE II Thin Clouds, MLS 146 hPa and 100 hPa Water Vapor and CO, NCEP Tropopause Temperature, and GEIA CO Surface Emission Shown in Figure 2[a]

|	TRMM 210 K Cloud	TRMM 20 dBZ at 14 km	SAGE II Cloud 14–16 km	SAGE II Cloud 16–18 km	MLS Water Vapor at 146 hPa	MLS Water Vapor at 100 hPa	MLS CO at 146 hPa	MLS CO at 100 hPa	CO Surface Emission	NCEP Tropo T
210K cloud	1	**0.61**	**0.52**	**0.51**	**0.60**	−0.34	0.31	0.27	0.07	−0.49
20 dBZ at 14 km	**0.61**	1	0.3	0.33	0.46	−0.08	**0.60**	0.46	0.37	−0.19
SAGE II cld 14−16 km	**0.52**	0.3	1	0.45	0.47	−0.29	0.21	0.24	0.13	−0.46
SAGE II cld 16−18 km	**0.51**	0.33	0.45	1	**0.54**	**−0.61**	0.17	0.41	0.04	**−0.69**
MLS 146 hPa H2O	**0.60**	0.46	0.47	**0.54**	1	−0.41	0.44	0.48	0.26	**−0.57**
MLS 100 hPa H2O	−0.34	−0.08	−0.29	**−0.61**	−0.41	1	−0.12	**−0.54**	0.06	**0.81**
MLS 146 hPa CO	0.31	**0.60**	0.21	0.17	0.44	−0.12	1	**0.69**	0.40	−0.14
MLS 100 hPa CO	0.27	0.46	0.24	0.41	0.48	**−0.54**	**0.69**	1	0.22	**−0.50**
CO surface emission	0.07	0.37	0.13	0.04	0.26	0.06	0.40	0.22	1	0.08
NCEP tropopause T	−0.49	−0.19	−0.46	**−0.69**	**−0.57**	**0.81**	−0.14	**−0.50**	0.08	1

[a]Large values are shown in bold.

the fact that deep convection moistens the upper troposphere. However, the banded signal in deep convection is very weak in 100 hPa water vapor. The exceptions are the dry air over the west Pacific, and Africa, and Amazon in February. Water vapor at 100 hPa is correlated, however, with tropopause temperature (Figure 2i). There are three cold tropopause temperature bands, located over the west Pacific, Africa, and the Amazon.

[11] Deep convection is also correlated with CO at 146 hPa, except in the west Pacific region. The concentrations appear to be related to deep convective transport of CO from primary sources of biomass burning [*Duncan et al.*, 2003]. Note that CO surface emission is particularly high over Africa in January and July, and over the Amazon in August (Figure 2j). A similar geo-seasonal pattern in CO is seen at 100 hPa (Figure 2h), although concentrations are high over the entire tropics in May, June, and December, perhaps due to horizontal transport.

[12] Values of the geo-seasonal correlation coefficients between each of the variables shown in Figure 2 are listed in Table 1. The highest correlation (0.81) is between 100 hPa water vapor and tropopause temperature. There is also high correlation between the SAGE II thin cloud at 16–18 km and the tropopause temperature (0.69), and between SAGE II thin cloud at 16–18 km and water vapor at 100 hPa (−0.61). However, SAGE II thin clouds at the lower 14–16 km layer are more closely related with the deep convection represented by cold 210 K clouds (0.52). High correlation also exists between 146 hPa CO and 20 dBZ radar echoes reaching 14 km (−0.69).

4. Discussion

[13] On the basis of the geo-seasonal variation patterns shown in Figure 2 and the correlation values listed in Table 1, we may generally divide the observed parameters into two
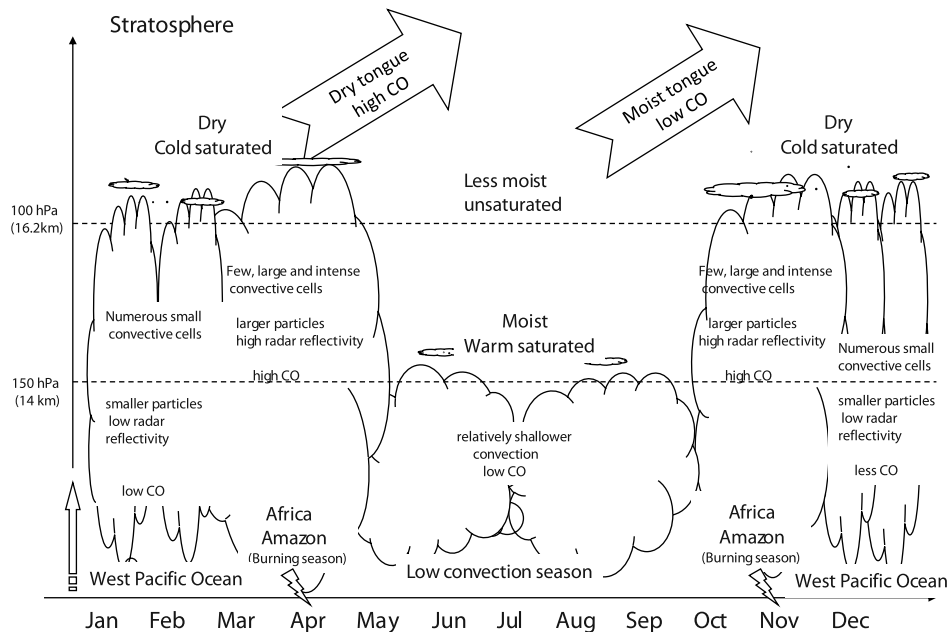
Figure 3. Schematic diagram of processes controlling the seasonal cycle in water vapor and CO near the tropical tropopause.

groups. The first group includes thin clouds in the 14–16 km layer, CO at 146 hPa and 100 hPa, and water vapor at 146 hPa. Each of these parameters correlates highly with amount of tropical deep convection reaching near the tropopause, if not necessarily its intensity. The second group of parameters includes the water vapor concentration at 100 hPa, thin clouds in the 16 to 18 km layer, and tropopause temperature. Our explanation for why these atmospheric variables fall into two groupings is as follows. Deep convection transports water vapor and CO to 146 hPa. However, only CO is further transported by convection to 100 hPa. The mixing ratio of water vapor decreases greatly during its upward transport from 146 hPa to 100 hPa. While we cannot ascertain whether the upward transport is through deep convection, by large scale ascent, or both at the same time, the decrease in water vapor concentration is well explained by the depression in tropopause temperature.

[14] Figure 3 shows a schematic diagram of the physical processes that are consistent with the above hypothesis. In December, January and February, deep convection over the west Pacific is abundant but relatively weak (figure not shown). It transports high concentrations of water vapor but low concentrations of CO to near the tropopause. Ascent of the water vapor through the cold tropopause dehydrates the air to form the stratospheric dry tongue in the water vapor tape recorder. In March, April, and May, a small number of large and intense convective events over Africa and the Amazon penetrate the tropopause [*Liu and Zipser*, 2005]. They transport large amounts of CO to the tropical tropopause from surface sources of biomass burning. This is different from the explanation of the CO peak by Indochina source from model results [*Schoeberl et al.*, 2006]. This air is freeze-dried following passage through the cold tropopause. From June to early September, tropical convection is common, but it is relatively weak compared to other times of the year, and it reaches lower altitudes. Also, the tropopause is warmer. This enables more tropospheric moisture to pass through to the stratosphere and form the moist tongue. CO emission at the surface is high, but because deep convection is weak, relatively low quantities of CO reach the tropopause. Beginning in late September, strong deep convection resumes over Amazon and Africa and tropopause temperature decreases. Dry air with high CO levels transits through the tropopause and it forms a dry tongue again with high CO. The result is that water vapor at 100 hPa has an annual cycle, but CO at 100 hPa has a semi-annual cycle.

[15] There are several concerns regarding the results and discussions in this study.

[16] 1. Some of the parameters used are only proxies for physical processes. For example, 210 K cloud area is used to represent deep convective vertical transport rather than convective mass flux.

[17] 2. Because of sampling problems, in particular with SAGE II, only a coarse geo-seasonal grid is used.

[18] 3. Coarse vertical resolutions of MLS water vapor and CO retrievals are another concern.

5. Summary

[19] Using several independent satellite datasets, the geo-seasonal variations of deep convection, thin clouds, water vapor and CO near tropical tropopause are compared. There is high correlation between deep convection and thin clouds near the tropopause. However, the geo-seasonal pattern of tropopause temperature has high correlation with thin clouds as well. An annual cycle of water vapor above tropopause may be explained by a "freeze and dry" process that is controlled by the seasonal variation of tropopause temperature. A semi-annual cycle of CO is explained by seasonal variations in deep convective transport and biomass burning.

References

Alcala, C. M., and A. E. Dessler (2002), Observations of deep convection in the tropics using the Tropical Rainfall Measuring Mission (TRMM) precipitation radar, *J. Geophys. Res.*, *107*(D24), 4792, doi:10.1029/2002JD002457.

Brewer, A. M. (1949), Evidence for a world circulation provided by the measurements of helium and water vapor distribution in the stratosphere, *Q. J. R. Meteorol. Soc.*, *75*, 351–363.

Danielsen, E. F. (1982), A dehydration mechanism for the stratosphere, *Geophys. Res. Lett.*, *9*, 605–608.

Dessler, A. E., S. P. Palm, W. D. Hart, and J. D. Spinhirne (2006), Tropopause-level thin cirrus coverage revealed by ICESat/Geoscience Laser Altimeter System, *J. Geophys. Res.*, *111*, D08203, doi:10.1029/2005JD006586.

Duncan, B. N., R. V. Martin, A. C. Staudt, R. Yevich, and J. A. Logan (2003), Interannual and seasonal variability of biomass burning emissions constrained by satellite observations, *J. Geophys. Res.*, *108*(D2), 4100, doi:10.1029/2002JD002378.

Gettelman, A., M. L. Salby, and F. Sassi (2002), Distribution and influence of convection in the tropical tropopause region, *J. Geophys. Res.*, *107*(D10), 4080, doi:10.1029/2001JD001048.

Hartmann, D. L., J. R. Holton, and Q. Fu (2001), The heat balance of the tropical tropopause, cirrus, and stratospheric dehydration, *Geophys. Res. Lett.*, *28*, 1969–1972.

Holton, J. R., and A. Gettelman (2001), Horizontal transport and the dehydration of the stratosphere, *Geophys. Res. Lett.*, *28*, 2799–2802.

Jensen, E., and L. Pfister (2004), Transport and freeze-drying in the tropical tropopause layer, *J. Geophys. Res.*, *109*, D02207, doi:10.1029/2003JD004022.

Jensen, E. J., O. B. Toon, H. B. Selkirk, J. D. Spinhirne, and M. R. Schoeberl (1996), On the formation and persistence of subvisible cirrus clouds near the tropical tropopause, *J. Geophys. Res.*, *101*, 21,361–21,376.

Kar, J., et al. (2004), Evidence of vertical transport of carbon monoxide from Measurements of Pollution in the Troposphere (MOPITT), *Geophys. Res. Lett.*, *31*, L23105, doi:10.1029/2004GL021128.

Kent, G. S., D. M. Winker, M. T. Osborn, and K. M. Skeens (1993), A model for the separation of cloud and aerosol in SAGE II occultation data, *J. Geophys. Res.*, *98*, 20,725–20,735.

Kistler, R., et al. (2001), The NCEP-NCAR 5-year reanalysis: Monthly means CD-ROM and documentation, *Bull. Am. Meteorol. Soc.*, *82*, 247–267.

Kummerow, C., W. Barnes, T. Kozu, J. Shius, and J. Simpson (1998), The tropical rainfall measuring mission (TRMM) sensor package, *J. Atmos. Oceanic Technol.*, *15*, 809–817.

Liu, C. (2007), Geographical and seasonal distribution of tropical tropopause thin clouds and their relation to deep convection and water vapor viewed from satellite measurements, *J. Geophys. Res.*, doi:10.1029/2006JD007479, in press.

Liu, C., and E. J. Zipser (2005), Global distribution of convection penetrating the tropical tropopause, *J. Geophys. Res.*, *110*, D23104, doi:10.1029/2005JD006063.

Liu, C., E. J. Zipser, and S. W. Nesbitt (2007), Global distribution of tropical deep convection: Different perspectives using infrared and radar as the primary data source, *J. Clim.*, *20*, 489–503.

Livesey, N. J., et al. (2005), Earth Observing Systems (EOS) Microwave Limb Sounder (MLS) version 1.5 level 2 data quality and description document, Version 1.51, internal document, Jet Propul. Lab., Pasadena, Calif.

Livesey, N. J., W. V. Snyder, W. G. Read, and P. A. Wagner (2006), Retrieval algorithms for the EOS Microwave Limb Sounder (MLS) instrument, *IEEE Trans. Geosci. Remote Sens.*, *44*, 1144–1155.

Massie, S., A. Gettelman, W. Randel, and D. Baumgardner (2002), Distribution of tropical cirrus in relation to convection, *J. Geophys. Res.*, *107*(D21), 4591, doi:10.1029/2001JD001293.

McCormick, M. P., E. W. Chiou, L. R. McMaster, W. P. Chu, J. C. Larsen, D. Rind, and S. Oltmans (1993), Annual variation of water vapor in the stratosphere and upper troposphere observed by the Stratospheric Aerosol and Gas Experiment II, *J. Geophys. Res.*, *98*, 4867–4874.

McCormick, M. P., L. W. Thomason, and C. R. Trepte (1995), Atmospheric effects of the Mt. Pinatubo eruption, *Nature*, *373*, 399–404.

McFarquhar, G. M., A. J. Heymsfield, J. Spinhirne, and B. Hart (2000), Thin and subvisual tropopause tropical cirrus: Observations and radiative impacts, *J. Atmos. Sci.*, *57*, 1841–1853.

Mote, P. W., K. H. Rosenlof, M. E. McIntyre, E. S. Carr, J. C. Gille, J. R. Holton, J. S. Kinnersley, H. C. Pumphrey, J. M. Russell III, and J. W. Waters (1996), An atmospheric tape recorder: The imprint of tropical tropopause temperature on stratospheric water vapor, *J. Geophys. Res.*, *101*, 3989–4006.

Newell, R. E., and S. Gould-Stewart (1981), A strastoperic fountain?, *J. Atmos. Sci.*, *38*, 2789–2796.

Randel, W. J., F. Wu, S. J. Oltmans, K. Rosenlof, and G. E. Nedoluha (2004), Interannual changes of stratospheric water vapor and correlations with tropical tropopause temperatures, *J. Atmos. Sci.*, *61*, 2133–2148.

Read, W. G., D. L. Wu, J. W. Waters, and H. C. Pumphrey (2004), A new 147–56 hPa water vapor product from the UARS Microwave Limb Sounder, *J. Geophys. Res.*, *109*, D06111, doi:10.1029/2003JD004366.

Sandor, B. J., E. J. Jensen, E. M. Stone, W. G. Read, J. W. Waters, and J. L. Mergenthaler (2000), Upper troposphereic humidity and thin cirrus, *Geophys. Res. Lett.*, *27*, 2645–2648.

Schoeberl, M. R., B. N. Duncan, A. R. Douglass, J. Waters, N. Livesey, W. Read, and M. Filipiak (2006), The carbon monoxide tape recorder, *Geophys. Res. Lett.*, *33*, L12811, doi:10.1029/2006GL026178.

Sherwood, S. C., and A. E. Dessler (2000), On the control of stratospheric humidity, *Geophys. Res. Lett.*, *27*, 2513–2516.

Su, H., W. G. Read, J. H. Jiang, J. W. Waters, D. L. Wu, and E. J. Fetzer (2006), Enhanced positive water vapor feedback associated with tropical deep convection: New evidence from Aura MLS, *Geophys. Res. Lett.*, *33*, L05709, doi:10.1029/2005GL025505.

Wang, P. H., P. Minnis, M. P. McCormick, G. S. Kent, and K. M. Skeens (1996), A 6-year climatology of cloud occurrence frequency from stratospheric aerosol and gas experiment II observations (1985–1990), *J. Geophys. Res.*, *101*, 29,407–29,429.

———————————

T. Garrett, C. Liu, and E. Zipser, Department of Meteorology, University of Utah, Salt Lake City, UT 84112, USA. (liuct@met.utah.edu)

J. H. Jiang and H. Su, JPL, California Institute of Technology, Pasadena, CA 91109, USA.